Click Here for Full Article

Ocean climate change fingerprints attenuated by salt fingering?

Gregory C. Johnson[1] and Kelly A. Kearney[2]

[1] Intensified double diffusive mixing may attenuate changes in ocean temperature and salinity patterns from global-warming induced increases in the Earth's hydrological cycle. Increasingly fresher Antarctic Intermediate Water and saltier subtropical waters would tend to increase destabilizing vertical salinity stratification compared to the stabilizing temperature stratification. Destabilization would increase salinity (and temperature) fluxes through double-diffusive salt fingering. These fluxes could in turn act to reduce widely recognized climate change fingerprints, potentially leading to underestimates of ocean changes in climate studies that do not account for double-diffusive mixing. Data from a subtropical trans-Indian Ocean survey occupied in 1987, 1995, 2002, and 2009 are used to investigate temperature-salinity changes and to estimate the variations of double diffusive mixing driven by these changes. **Citation:** Johnson, G. C., and K. A. Kearney (2009), Ocean climate change fingerprints attenuated by salt fingering?, *Geophys. Res. Lett.*, *36*, L21603, doi:10.1029/2009GL040697.

1. Introduction

[2] Global warming models suggest that the hydrological cycle increases as the atmosphere warms and carries more moisture, and indicate that precipitation and evaporation increases should be detectable by the late 20th century [*Held and Soden*, 2006]. Evaporation dominates over precipitation in the subtropical oceans, yielding salty surface conditions, whereas precipitation exceeds evaporation in the subpolar regions, yielding fresher surface conditions [*Béranger et al.*, 1999]. A hydrological cycle increase should lead to even saltier subtropical and fresher subpolar surface waters.

[3] Since ocean waters move primarily along constant potential density, σ_θ, surfaces, these warmer and saltier subtropical waters overlie colder and fresher subpolar waters in mid-latitudes, with the vertical temperature gradient stabilizing the water column and the vertical salinity gradient partially destabilizing it. In this portion of the water column, the Central Water (CW), the potential temperature–salinity ($\theta-S$) relation is not linear, with curvature caused by mixing associated with salt fingering, a double-diffusive instability [*Schmitt*, 1981]. The $\theta-S$ curve tends toward constant density ratio, $R_\rho = -\alpha\partial_z\theta/\beta\partial_z S$, where α is the thermal expansion coefficient and β the haline contraction coefficient. When $R_\rho < 2$, the larger molecular diffusivity of temperature relative to salinity results in salt fingering

[*Schmitt*, 1981]. As R_ρ approaches 1, salt fingering strengthens, as does diffusion of salt, and to a lesser extent, temperature [*St. Laurent and Schmitt*, 1999].

[4] Cooling and freshening of subpolar waters on isopycnals and warming and salinification of subtropical waters on shallower overlying isopycnals over the last several decades has been reported in the Atlantic [*Curry et al.*, 2003], Pacific [*Wong et al.*, 1999], and South Indian [*Bindoff and McDougall*, 2000] Oceans. Such changes in these water masses below and above the CW will tend to rotate the $\theta-S$ curve clockwise within it, toward closer alignment with isopycnals. Such rotation decreases R_ρ, increases salt fingering, hence salinity and temperature fluxes, and possibly moderates the changes in interior ocean water property signatures imparted at the surface by rotating the $\theta-S$ curve counterclockwise back toward higher R_ρ. We examine this hypothesis in the South Indian Ocean, although partial reverses to the upper water column salinification there [*Bryden et al.*, 2003] do complicate the story.

2. Data and Methods

[5] We analyze data along a trans-Indian Ocean section from Africa to Australia sampled nominally along 32°S (Figure 1a). Three full occupations of this section use Conductivity-Temperature-Depth (CTD) instruments that provide accurate and continuous vertical profiles of T and S at 2-dbar pressure (P) intervals: in Nov.–Dec. 1987 [*Toole and Warren*, 1993], Mar.–Apr. 2002 [*McDonagh et al.*, 2008], and Mar.–May 2009. The western portion was also occupied in Jun.–Jul. 1995 [*Donohue and Toole*, 2003] and the eastern portion in Mar.–Apr. 1995 [*Talley and Baringer*, 1997].

[6] Profiles of T and S are low-passed vertically in P space with a 39-point Hanning filter. Turner angle, (Tu), a measure of water column stability related to R_ρ [*Ruddick*, 1983], θ, and σ_θ are calculated from the filtered T and S data. These quantities are then put on regular grids for all sections, both pressure-longitude, and potential density anomaly-longitude, using linear interpolation. While R_ρ is intuitive, it is also non-linear and discontinuous; therefore we work with Tu and convert to R_ρ for discussion and display.

[7] Argo profiles of T and S versus P used here were downloaded in September 2009. Some profiles have only automated real-time quality control applied, and some are delayed mode quality controlled. All data labeled as "good" are used here, over 496,000 profiles globally. Profiles per year grew from ∼500 in 1999 to ∼93,000 in 2008.

[8] Mixed layer S, θ, and σ_θ are estimated from each profile's sample closest to 10 dbar, but always between 4 and 25 dbar. Mixed layer P is estimated as the P at which the linearly interpolated σ_θ of each profile exceeds the

---
[1]Pacific Marine Environmental Laboratory, NOAA, Seattle, Washington, USA.
[2]Department of Geosciences, Princeton University, Princeton, New Jersey, USA.

surface value by 0.03 kg m^{-3}, discarding values interpolated over too large an interval. These quantities are mapped on a 1° × 1° grid at monthly intervals using a 3-dimensional loess filter (a weighted least-squares quadratic fit) with a 500-km meridional scale, a 1000-km zonal scale, and a 2-month time scale (disregarding year), discarding extreme outliers.

[9] Similarly, for each profile, θ, S, and P data are interpolated to a fixed set of σ_θ levels, again discarding data interpolated over too large pressure intervals and extreme outliers. Retained data are mapped at each density level to a 1° × 1° grid using a 2-D loess spatial filter (same length scales as above).

3. Results

[10] South Indian Ocean CW θ and S distributions on σ_θ horizons are quite homogenous, as typified by S on $\sigma_\theta =$ 26.75 kg m^{-3}, with near-uniform values between about 35°S and 15°S (Figure 1a) bracketed by fresh influences of the Indonesian Throughflow to the north and the sub-Antarctic regions to the south. Fresher Antarctic Intermediate Water (AAIW, $\sigma_\theta \sim 27.2$ kg m^{-3}) spreads northward overlain by the much saltier subtropical waters ($\sigma_\theta < 26$ kg m^{-3}), with the strong destabilizing vertical salinity gradient characteristic of CW between these two water masses (Figure 1b). South Indian Ocean Sub-Antarctic Mode Water (SAMW) [*Wong*, 2005] sits within the CW, as evinced by the very thick layer of relatively uniform density around $\sigma_\theta =$ 26.75 kg m^{-3} that spreads northwestward from its origin along the winter outcrop of that isopycnal (Figure 1c).

[11] The repeat trans-Indian Ocean sections along 32°S sample the southern CW well. The CW is roughly bounded by 26.3 < σ_θ < 27.1 kg m^{-3} (or 16 > θ > 6°C), where R_ρ is relatively low (Figure 2a). Here R_ρ has a local vertical minimum, weaker and deeper in the west ($R_\rho \sim 2.3$ near 600 dbar in 1987) and stronger and shallower in the east ($R_\rho \sim 1.5$ around 300 dbar in 1987). These eastern low values indicate conditions conducive to vigorous salt fingering [*Schmitt*, 1981], hence high vertical diffusivity [*St. Laurent and Schmitt*, 1999].

[12] The differences of the 1987 longitude-pressure section of R_ρ and any of those from the subsequent full or partial sections, for example 2009–1987 (Figure 2b), suggests that the R_ρ minimum has either intensified or deepened, and sometimes both, since 1987. Below its minimum and sometimes within it in the west, R_ρ generally decreases, with declines of around 0.2 or more typical near 800 dbar in the west and 700 dbar in the east. Above the minimum, and sometimes within it in the east, increases of a similar magnitude are evident in the 2009 R_ρ field (and those from other years) when compared with the 1987 values.

[13] The longitudinal variation in R_ρ, as well as the availability of 1995 data only at the eastern and western ends of the 32°S section, prompt a three-sector analysis:
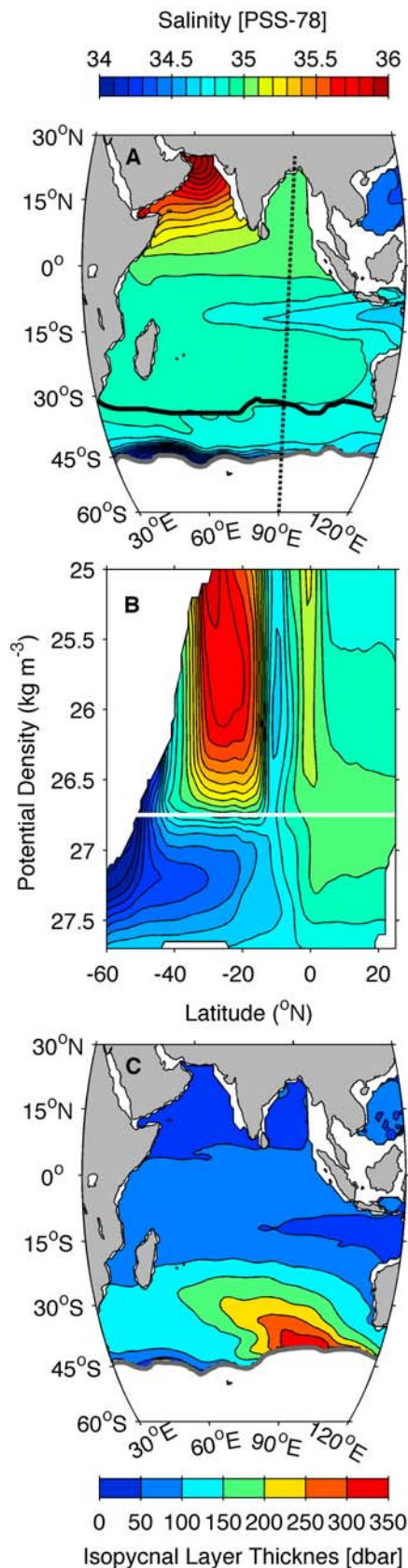
Figure 1. (a) Salinity (S) map on potential isopycnal $\sigma_\theta =$ 26.75 kg m^{-3} from Argo data color contoured at 0.1 PSS-78 intervals (top color bar) with locations of 2009 trans-Indian Ocean section (black line), Figure 1b meridional transect (dashed line), and winter isopycnal outcrop (grey line). (b) Latitude-σ_θ section of S contoured at 0.1 PSS-78 intervals (top color bar) along 90°E with values lighter than wintertime surface densities masked and $\sigma_\theta = 26.75$ kg m^{-3} (white line) used in Figure 1a indicated. (c) Map of thickness of the layer 26.7 < σ_θ < 26.8 kg m^{-3} from Argo data color contoured at 50-dbar intervals (bottom color bar).
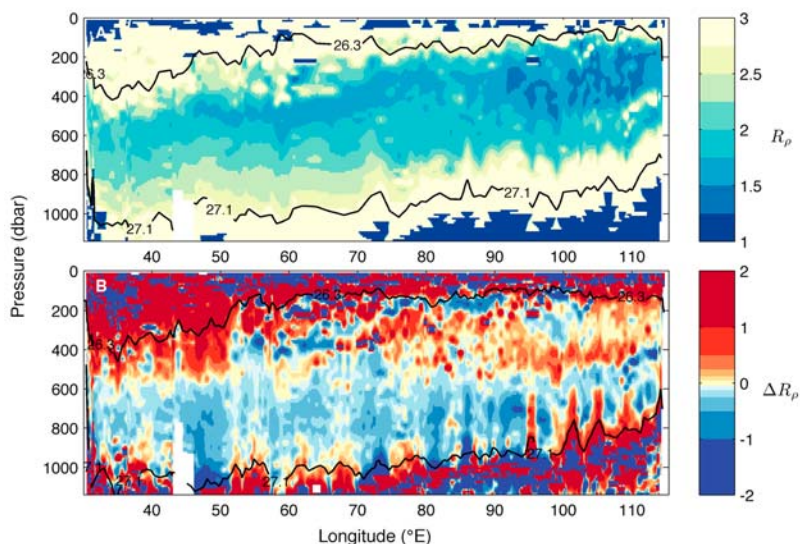
Figure 2. (a) Longitude-pressure section of density ratio (R_ρ) estimated from data from the 1987 occupation of a trans-Indian Ocean section along nominal latitude 32°S (see Figure 1a for location). Potential isopycnals $\sigma_\theta = 26.3$ and 27.1 kg m^{-3} approximately bounding the Central Water (CW) are indicated by black contours. Only a limited portion of the $-\infty$ to ∞ range of R_ρ is differentiated here. (b) Section of 2009–1987 difference of density ratio (ΔR_ρ) with these same isopycnals, but for 2009, indicated by black contours. Large R_ρ differences outside the CW occur where R_ρ tends to have large absolute values (where the vertical salinity gradient is small).

western (Africa–50°E), central (50°E–80°E), and eastern (80°E–Australia). Furthermore, since ocean waters move primarily along σ_θ, quantities discussed are averaged within these sectors on σ_θ rather than P surfaces.

[14] All three sectors display classic CW characteristics, with saltier (and though not shown, warmer) water overlying fresher (and colder) water (Figures 3a–3c). The denser portions of the CW grow fresher (and, by definition, colder)

on isopycnals with time in all of the sectors, consistent with global warming scenarios. In contrast, changes in the lighter portions of the water column are not as monotonic, as previously noted [*Bryden et al.*, 2003]. The 2002 section is warmer and saltier on isopycnals in the upper portion of the water column relative to the other sections, except in the eastern sector, where no single section has that distinction. However, in the eastern sector the section latitudes also
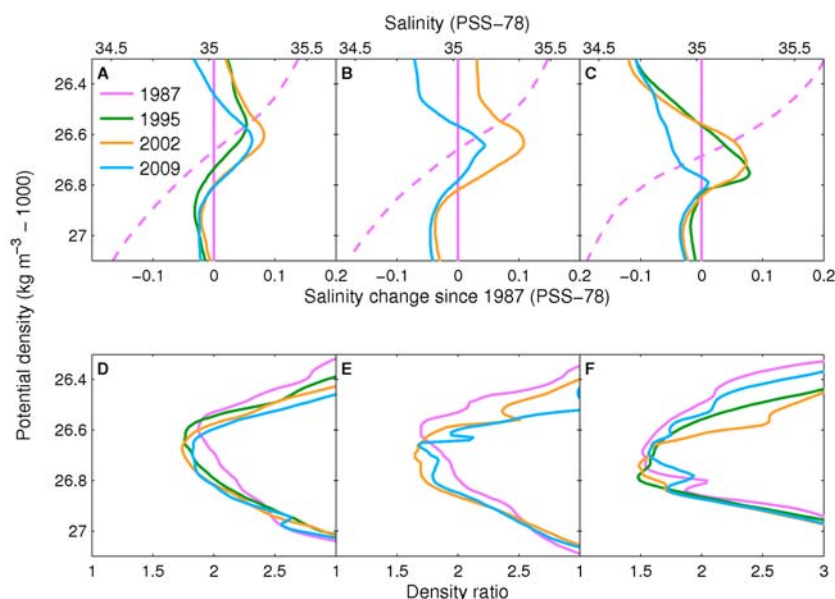
Figure 3. (a–c) The 1987 Salinity – potential density ($S-\sigma_\theta$) curves (bottom scale, dashed line) with S anomalies from that curve from latter years (top scale, solid lines). Colors indicate years (legend). Data from the three complete and one partial modern occupations of the trans-Indian Ocean section nominally along 32°S are used. (d–f) Averages of R_ρ on σ_θ surfaces for each year. Longitude ranges span western (Africa–50°E; Figures 3a and 3d), central (50°E–80°E; Figures 3b and 3e), and eastern (80°E–Australia; Figures 3c and 3f) sectors of the section.
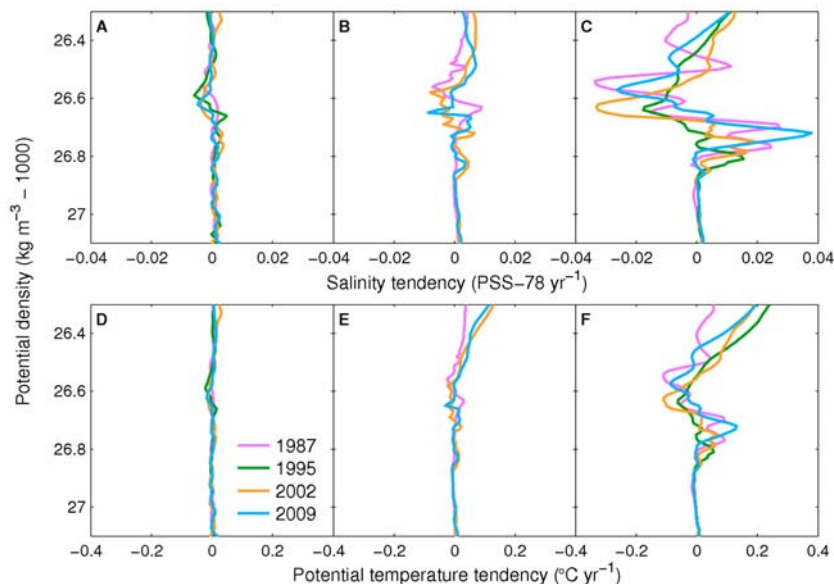
Figure 4. (a–c) Average vertical salinity tendencies (PSS-78 yr^{-1}) on σ_θ horizons with colors indicating years (legend) estimated by applying a diffusivity parameterization to data from the three complete and one partial modern occupations of a trans-Indian Ocean section nominally along 32°S. (d–f) Analogous averages of vertical potential temperature tendencies (°C yr^{-1}). Longitude ranges span the western (Africa–50°E; Figures 4a and 4d), central (50°E–80°E; Figures 4b and 4e), and eastern (80°E–Australia; Figures 4c and 4f) sectors of the section.

differ by as much as a few degrees among the individual years. Since more northerly stations will generally sample warmer, saltier subtropical waters, some of the differences in the eastern sector may be spatial, and not temporal.

[15] R_ρ is a sensitive indicator of changes in the $\theta-S$ relations, being constructed from vertical derivatives (Figures 3d–3f). The R_ρ minima (at $26.6 < \sigma_\theta < 26.8$ kg m^{-3} or $13.3 > \theta > 9.4°$C) are least extreme in the western sector, with values just below 2.0, suggesting only marginal propensity toward salt fingering and consequent elevated mixing [*Schmitt*, 1981; *St. Laurent and Schmitt*, 1999]. However, the R_ρ minimum in the western sector moves toward generally denser horizons and strengthen slightly from 1987 at least through 2002, suggesting the possibility of more mixing with time there owing to freshening and cooling AAIW influences from below, as well as warming and salinification above, albeit with a partial return to a weaker minimum in 2009. In the central sector, the R_ρ minimum is stronger than in the west, near 1.6, suggesting stronger salt fingering activity. It again moves to denser horizons from 1987 to 2002 in the central sector, staying roughly fixed between 2002 and 2009. In the eastern sector, the R_ρ minimum is strongest and on densest horizons, approaching 1.5 on average, with no consistent pattern of change in either strength or isopycnal level among the four occupations of the section. This very low R_ρ minimum suggests quite strong salt fingering and elevated mixing in the eastern sector CW.

4. Discussion

[16] One possible interpretation of these patterns is that in the east where the propensity for salt fingering is strong in all years, changes in the CW $\theta-S$ properties may be rapidly moderated by strong vertical mixing, keeping the $\theta-S$ curves (and hence the associated values of R_ρ) relatively invariant in time. In the central region, where salt fingering is predicted weaker but still present, the cooling and freshening of the AAIW with time has moved the R_ρ minimum to denser horizons, but not strengthened it, so moderate mixing is working its way down toward the freshening and cooling AAIW. In the western region, where the R_ρ minimum is weakest, the changing AAIW has not only moved the R_ρ minimum to denser horizons, but also shifted that portion of the water column toward lower R_ρ values and hence a greater propensity for salt fingering since 1987, potentially moving toward moderation of the upper reaches of the AAIW changes. In contrast to the AAIW signal below the R_ρ minimum, the patterns above the R_ρ minimum are not monotonic, as previously reported for $\theta-S$ variations through 2002 [*Bryden et al.*, 2003]. The 32°S section is in a region of strong meridional $\theta-S$ gradients for $\sigma_\theta < 26.7$ kg m^{-3} (Figure 1b), and so may be too far south to detect best long-term changes in the subtropical salinity maximum.

[17] The effects of these R_ρ patterns and changes on mixing can be estimated by applying a diffusivity parameterization following *Johnson* [2006] to the data from each section to estimate vertical salt and temperature fluxes, and from those fluxes find tendencies, on density surfaces (Figure 4). These tendency estimates are noisy, but sector average patterns are still clear. In the western sector, the R_ρ minima are too weak in 1987 to effect any mixing over background levels; there is a slight tendency for salinification (and heating) for densities greater than the R_ρ minimum post-1987 and a slight tendency for freshening (and cooling) for densities less than the R_ρ minimum post-1987. In the central sector the tendency toward salinification and warming for densities greater than the R_ρ minimum and toward freshening and cooling at lighter densities is stronger. In the eastern sector the pattern is even stronger. These tendencies are highest on the edges of the SAMW, where property curva-

tures are elevated. Higher tendencies for $\sigma_\theta < 26.5$ kg m^{-3} in the eastern and central sections are associated with the seasonal thermocline, and will not be discussed further here.

[18] In the eastern sector the S and θ tendencies estimated within the CW can exceed ± 0.02 PSS-78 yr^{-1} and 0.1°C yr^{-1} (Figure 4). Salt and heat likely flux downward across $\sigma_\theta \sim 26.7$ kg m^{-3} but roughly cancel in their contributions to vertical density flux. These tendencies are on the order of rates of previously reported decadal changes in S and θ on isopycnals in the region [*Bindoff and McDougall*, 2000; *Bryden et al.*, 2003]. This result opens the possibility that salt-fingering-driven vertical mixing could moderate such climate signals, especially if freshening of subpolar waters and salinification of subtropical waters over time act to decrease R_ρ further. In the absence of salt-fingering, observed decadal changes might be larger.

[19] Interior changes in ocean properties such as θ and S can be useful in diagnosing climate changes at the ocean surface [*Bindoff and McDougall*, 1994] and are robust fingerprints of such global climate change in models [*Banks et al.*, 2000]. Ocean changes of salinity within isopycnal layers over the past few decades have been used to estimate the size of decadal increases in the hydrological cycle over the ocean (K. P. Helm et al., Global hydrological-cycle changes inferred from observed ocean salinity, submitted to *Nature Geoscience*, 2009). If these increases in the hydrological cycle increase the destabilizing salinity gradient and hence vertical mixing, as illustrated here especially for the AAIW changes below the R_ρ minimum, elevated vertical salt and temperature fluxes, as estimated here, may be of sufficient magnitude to moderate this climate signature imparted at the ocean surface as it travels into the interior by transferring increasing amounts of heat and salt downward across isopycnals, making layers that were cooled and freshened at the surface warmer and saltier in the interior, and vice versa. Hence, accounting for diapycnal processes like increased mixing owing to salt fingering in climate change studies could improve their diagnostic skill. At least one numerical model has demonstrated more realistic steady-state water-mass property distributions when a parameterization of double-diffusion is included [*Merryfield et al.*, 1999].

References

Banks, H., R. Wood, J. Gregory, T. Johns, and G. Jones (2000), Are observed decadal changes in intermediate water masses a signature of anthropogenic climate change?, *Geophys. Res. Lett.*, 27, 2961–2964, doi:10.1029/2000GL011601.

Béranger, K., L. Siefridt, B. Barnier, E. Garnier, and H. Roquet (1999), Evaluation of operational ECMWF surface freshwater fluxes of oceans during 1991–1997, *J. Mar. Syst.*, 22, 13–36, doi:10.1016/S0924-7963(99)00028-7.

Bindoff, N. J., and T. J. McDougall (1994), Diagnosing climate-change and ocean ventilation using hydrographic data, *J. Phys. Oceanogr.*, 24, 1137–1152, doi:10.1175/1520-0485(1994)024<1137:DCCAOV>2.0.CO;2.

Bindoff, N. J., and T. J. McDougall (2000), Decadal changes in an Indian Ocean Section at 32°S and their interpretation, *J. Phys. Oceanogr.*, 30, 1207–1222, doi:10.1175/1520-0485(2000)030<1207:DCAAIO>2.0.CO;2.

Bryden, H. L., E. L. McDonagh, and B. A. King (2003), Changes in ocean water mass properties: Oscillations or trends?, *Science*, 300, 2086–2088, doi:10.1126/science.1083980.

Curry, R., B. Dickson, and I. Yashavaev (2003), A change in the freshwater balance of the Atlantic Ocean over the past four decades, *Nature*, 426, 826–829, doi:10.1038/nature02206.

Donohue, K. A., and J. M. Toole (2003), A near-synoptic survey of the southwest Indian Ocean, *Deep Sea Res., Part II*, 50, 1893–1931, doi:10.1016/S0967-0645(03)00039-0.

Held, I. M., and B. J. Soden (2006), Robust response of the hydrological cycle to global warming, *J. Clim.*, 19, 5686–5699, doi:10.1175/JCLI3990.1.

Johnson, G. C. (2006), Generation and initial evolution of a mode water θ–S anomaly, *J. Phys. Oceanogr.*, 36, 739–751, doi:10.1175/JPO2895.1.

McDonagh, E. L., H. L. Bryden, B. A. King, and R. A. Saunders (2008), The circulation of the Indian Ocean at 32°S, *Prog. Oceanogr.*, 79, 20–36, doi:10.1016/j.pocean.2008.07.001.

Merryfield, W. J., G. Holloway, and A. E. Gargett (1999), A global ocean model with double-diffusive mixing, *J. Phys. Oceanogr.*, 29, 1124–1142, doi:10.1175/1520-0485(1999)029<1124:AGOMWD>2.0.CO;2.

Ruddick, B. (1983), A practical indicator of the stability of the water column to double-diffusive activity, *Deep Sea Res., Part A*, 30, 1105–1107, doi:10.1016/0198-0149(83)90063-8.

Schmitt, R. W. (1981), Form of the temperature-salinity relationship in the central water: Evidence for double-diffusive mixing, *J. Phys. Oceanogr.*, 11, 1015–1026, doi:10.1175/1520-0485(1981)011<1015:FOTTSR>2.0.CO;2.

St. Laurent, L., and R. W. Schmitt (1999), The contribution of salt fingers to vertical mixing in the North Atlantic Tracer Release Experiment, *J. Phys. Oceanogr.*, 29, 1404–1424, doi:10.1175/1520-0485(1999)029<1404:TCOSFT>2.0.CO;2.

Talley, L. D., and M. O. Baringer (1997), Preliminary results from WOCE hydrographic sections at 80°E and 32°S in the central Indian Ocean, *Geophys. Res. Lett.*, 24, 2789–2792, doi:10.1029/97GL02657.

Toole, J. M., and B. A. Warren (1993), A hydrographic section across the subtropical south Indian Ocean, *Deep Sea Res., Part I*, 40, 1973–2019, doi:10.1016/0967-0637(93)90042-2.

Wong, A. P. S. (2005), Subantarctic Mode Water and Antarctic Intermediate Water in the south Indian Ocean based on profiling float data 2000–2004, *J. Mar. Res.*, 63, 789–812, doi:10.1357/0022240054663196.

Wong, A. P. S., N. L. Bindoff, and J. A. Church (1999), Large-scale freshening of intermediate waters in the Pacific and Indian oceans, *Nature*, 400, 440–443, doi:10.1038/22733.

───────────────

G. C. Johnson, Pacific Marine Environmental Laboratory, NOAA, 7600 Sand Point Way NE, Bldg. 3, Seattle, WA 98115, USA. (gregory.c.johnson@noaa.gov)

K. A. Kearney, Department of Geosciences, Princeton University, Guyot Hall M70, Princeton, NJ 08544, USA.